EURASIP Journal on Advances in Signal Processing
a SpringerOpen Journal

RESEARCH Open Access

Performance of distributed beamforming for dense relay deployments in the presence of limited feedback information

Turo Halinen[1*], Alexis A Dowhuszko[1] and Jyri Hämäläinen[1,2]

Abstract

This paper studies the impact of quantized channel feedback on the performance of a (coherent) *distributed beamforming* (DBF) scheme. The analysis is done in the context of a wireless access network, and the goal is to provide an adequate broadband coverage for users located inside buildings. In the examined scenario, instead of trying to reach the serving *base station* (BS) directly, we assume that each mobile *user equipment* (UE) receives assistance from a cooperative group of network elements that is placed in close proximity (e.g., in the same room or office). This cluster of cooperative network elements is formed by a large number of low-cost *relaying stations* (RSs), which have fixed locations and are equipped with only one antenna. To simplify the analysis, communication in the first hop (i.e., from the mobile UE to the elements of the cluster) is assumed practically costless, making the bottleneck lie in the second hop of the system (i.e., from the elements of the cluster to the serving BS). Closed-form approximations for three different performance measures are derived (i.e., outage probability, ergodic capacity, bit error probability), providing accurate predictions of the fundamental limits that proposed system architecture is able to provide. Our analysis reveals that the achievable end-to-end performance when using a small amount of phase feedback information (per RS in the second hop) is very close to the full phase information upper bound, paving the way to the use of massive DBF architectures as a practical way to cope with high data rate demands of future wireless systems.

Keywords: Cooperative communications, Distributed beamforming, Decode-and-forward relays, Heterogeneous networks, Limited feedback information, Massive network element deployments, Non-perfect channel knowledge, Performance prediction

1 Introduction

The demand of mobile data has been growing at a steady pace in the last few years, as the usage of new types of mobile devices such as smartphones and tablets has become a mainstream. This tendency has been also fueled by the introduction of new mobile applications, creating a new category of users that call for a better support of high data rates. It is not surprising that many independent sources have predicted a dramatic increase in mobile broadband traffic in the next few years [1]. In addition, by the year 2020, it is also expected that every one of us will be surrounded by an average number of 10 wireless-enabled devices, resulting in a 10-fold increase in the number of equipment that will admit wireless connectivity (more than 50 billion connected devices are expected to be supported worldwide by the end of the decade) [2]. To cope with these demands, novel wireless network architectures will be required [3]. In line with this, one interesting option is based on deploying a large number of low-cost *relaying stations* (RSs) with fixed locations in hotspot areas of the mobile network (e.g., on walls and ceilings) [4]. The massive deployment of inexpensive RSs enables the implementation of a *distributed beam forming* (DBF) scheme, providing an improvement in the *signal-to-interference-plus-noise* power *ratio* (SINR) of the different end-to-end wireless connections (i.e., boosting the desired signal energy at the destination and mitigating the co-channel interference that is generated by neighbors).

*Correspondence: turo.halinen@aalto.fi
[1]Department of Communications and Networking, Aalto University, P.O. Box 13000, Aalto FI-00076, Finland
Full list of author information is available at the end of the article

Since the majority of voice calls and data usage sessions take place inside buildings by nomadic (mobile) users [5], the delivery of adequate indoor broadband coverage is crucial [6,7]. The provision of indoor broadband wireless access from macro-*base stations* (BSs) located outdoors is not a good option in practice: the high penetration losses caused by walls and floors put an indoor *user equipment* (UE) in a very disadvantageous situation (i.e., the energy consumption required for the signal transmission is increased, decreasing the amount of information that can be transferred effectively). For a customer that demands wireless connectivity in a small apartment or office, one possible solution is to deploy a low-power femto-/home BS and to provide connectivity to the core network of the service provider using, e.g., a residential digital subscriber line [8]. For corporate customers that demand an adequate broadband coverage in an office building, a hotel, or an airport, another option is to deploy a distributed architecture that relies on fiber optics (or power lines) to connect remote radio access units with a centralized processing unit [9,10]. In this work, a slightly different approach that combines concepts of the two previously described methods is considered: we focus on studying the performance of an indoor UE, when its transmitted signal is boosted by a massive cluster of cooperative network elements that are located in close proximity (i.e., in the same room or office) [4]. Such an approach is similar to the hierarchical cooperation scheme proposed in [11], when cooperation for long-range communications is only implemented inside the transmitting cluster. Compared to [12], we assume that the transmitting cooperative network is composed of a *large* number of fixed low-cost RSs (located in the walls and ceiling of the room) that enable the implementation of a distributed transmission in the link between the indoor UE (or main transmitter) and the macro-BS (or main receiver). Since the cost of deploying these RSs should be low by definition, the cooperative strategy that they can implement in practice is restricted to single-layer DBF with limited channel feedback information at the transmitter side.

The main idea behind DBF is simple: distribute the message within many disperse antenna elements and then coordinate the retransmission in the direction of the intended destination [13,14]. Unlike the aforementioned cases, we consider the implementation of a joint transmission scheme within the cluster of RSs that surrounds the main transmitter. In other words, we assume that an equivalent *distributed antenna system* (DAS) can be configured sharing a common message in the first hop (i.e., replacing wired links by almost costless wireless links due to close proximity) and implementing a DBF scheme with limited feedback in the second hop. Since it is assumed that the bottleneck of the system lies in the second hop, end-to-end performance can be improved, implementing a coherent transmission scheme from the cluster of RSs to the main receiver (i.e., adjusting the phases of the channel gains that the main receiver observes from each of the antenna elements that surrounds the main transmitter). This enables the coherent combination of the multiple replicas of the original message at the intended destination. The potential advantages of deploying a DBF architecture are well known in the literature: full diversity benefit and M-fold power gain for M active array elements in the network [15]. Note that to achieve the full diversity benefit, the inter-antenna separation in the second hop should be larger than the coherence distance of the channel; this is typically the case, e.g., when dealing with omnidirectional antennas in indoor environments with rich scattering (in this situation, the coherence distance is usually a fraction of the wavelength of the wireless system). We note that in the absence of *channel state information* (CSI) at the disperse antenna elements, the use of distributed space-time coding was also suggested, obtaining full diversity gains in the second hop [16].

The main challenges in our DBF scheme are the synchronization of *radio-frequency* carriers at the different RSs [17] and the estimation of each individual channel gain that the main receiver observes from each RS antenna in the second hop. An adaptive 1-bit feedback DBF algorithm that tries to solve these problems was developed by Mudumbai et al. in [18]. In the so-called Mudumbai's algorithm, random phase perturbations are applied independently in every disperse antenna element at each iteration, but only those phase perturbations that improve the received *signal-to-noise* power *ratio* (SNR) at the main receiver are retained. Even though Mudumbai's algorithm is simple to implement in practice, in this paper, we take a slightly different approach. We assume that the main receiver has the capability to estimate the phases of individual channel gains from each RS antenna in the second hop, using an N-bit uniform quantizer. This assumption is in line with different usage cases that are currently under study in 3GPP standardization, where the cellular network is proposed to assist a very large number of wireless-enabled devices and carry out control duties in, e.g., device-to-device communications [19].

Since the locations of RSs (and main receiver) are assumed fixed during the whole duration of the communication, the movement of scatterers is expected to be the only source of time selectivity in the corresponding channel gains; as a result, the coherence time of the wireless channels for the second hop are expected to be much larger than the signaling delay. Phase portions of the channel gains are assumed to take random (unknown) values at the beginning of the beamforming configuration process (with identical average SNR values for each individual channel gains), and signaling information is considered to be reported

on a per-RS basis along a proper time span (proportional to the coherence time of the wireless channel) that keeps the cost of control mechanisms at reasonable levels. To complement the research presented in [4], in this work, we study the effect of limited phase feedback information, deriving closed-form approximations to characterize three different physical layer performance measures: outage probability, ergodic capacity (i.e., mean achievable data rate), and bit error probability. Based on the presented analysis, we conclude that a relatively small amount of phase signaling information (i.e., $N = 3$ phase feedback bits per individual antenna) is sufficient to obtain a performance close to the one observed in the case of perfect channel phase information in the second hop.

The rest of the paper is organized as follows. Section 2 presents the system model, the assumptions on the limited feedback DBF algorithm, and the details of the performance criterion that will be used to carry out the analysis. Section 3 provides a closed-form expression for the probability distribution function of the received SNR of the system and then extends to the analysis of different performance measures. Section 4 presents numerical results that measure the effect of both the amount of feedback bits per channel and the number of network elements in the selected performance criteria. Finally, conclusions are drawn in Section 5. To facilitate the reading, most frequently used abbreviations are listed in the 'Abbreviations' section.

2 System model

The layout of our cooperative relaying system is illustrated in Figure 1. The system consists of a main transmitter, a main receiver, and a cluster of M active RSs (in fixed positions) that provides the array elements of the DBF scheme that is implemented in the second hop. All devices are equipped with a single transmit/receive antenna. In our system model, the main transmitter and the RSs in the cluster operate in half-duplex mode, in a *decode-and-forward* (DF) fashion. Thus, during the first hop of duration T_1, the message intended for the main receiver is sent from the main transmitter to the nearby array elements (i.e., the antennas of the distributed RSs). During the second hop of duration T_2, the message is sent from the array elements to the main receiver. It is assumed that the array elements share the same physical location with the main transmitter (e.g., same room or office). The average (distance-dependent) path loss attenuations in the links of the first hop are assumed to be small, and channel gains are either considered static or slowly varying (e.g., line-of-sight channel model). This makes it possible to assume that communication in the first link can be accomplished with (almost) no cost in terms of power and/or time (i.e., $T_1 \ll T_2$). However, if the array elements were distributed in different locations with respect to the main transmitter (e.g., in different rooms), the penetration losses caused by the walls and floors would increase the cost of communication in the first hop. Nevertheless, the longer distance that would typically exist between the clustered array elements and the main receiver in our proposed indoor-to-outdoor channel model implies a larger average path loss attenuations in the links of the second hop when compared with the ones of the first hop. In addition, it is also reasonable to consider that the chance of having a *line-of-sight* (LoS) connection is much lower in the second hop when compared with the probability of having a LoS link in the first one. All these assumptions make the second hop the bottleneck of the system; so, its analysis is the main objective of this paper. Particularly, we focus on the forward direction of the communication link (i.e., from main transmitter to main receiver) due to, as opposed to the main receiver, transmit power of RSs should be kept low to reduce their deployment cost as much as possible.

As depicted in Figure 1, a low-rate, reliable, and delay-free feedback channel exists between the main receiver and the elements of the disperse antenna array (i.e., the cluster of RSs). The main receiver uses this feedback channel to convey the quantized phase adjustment that each element of the antenna array should apply in transmission to maximize the SNR in reception. In other words, the limited feedback information that the main receiver reports is used to establish a DAS in the second hop. Multiple active array elements transmit cooperatively at the same time, focusing the resulting beam towards the direction of the intended destination over the second hop.

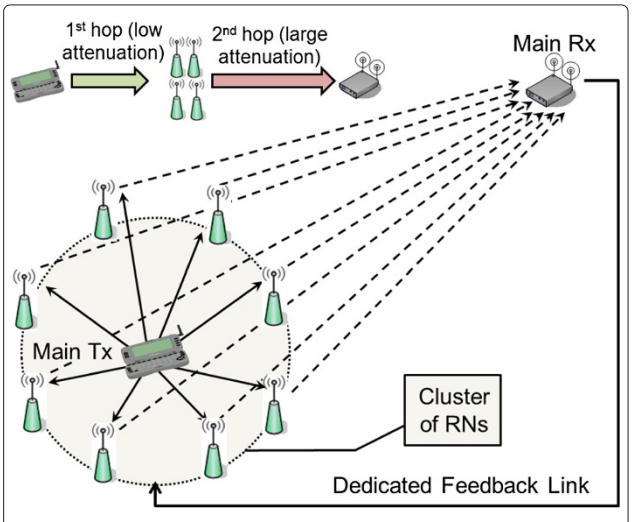

Figure 1 Generalized system model composed of a main transmitter, main receiver, and cluster of relaying network elements. The feedback link between main receiver and relaying cluster (around main transmitter) enables the implementation of a distributed beamforming scheme in the second hop.

Based on the model presented above, the signal that the main receiver experiences (in a spectrum portion with a flat frequency response) at transmission time interval i attains the following (dot product) form:

$$r[\,i] = (\mathbf{h}[\,i] \cdot \mathbf{x}[\,i]\,) + n = (\mathbf{h}[\,i] \cdot \mathbf{w}[\,i]\,)\; s + n, \tag{1}$$

where $\mathbf{x}[\,i] = (x_1[\,i] \ldots x_M[\,i]\,)$ is a row vector that contains the transmitted signals in the second hop (one per element in the cluster of RSs), $\mathbf{h}[\,i] = (h_1[\,i] \ldots h_M[\,i]\,)$ is the aggregate row channel vector (with zero-mean complex Gaussian coefficients) that contains the channel gains from each RS to the common receiver, and n is *additive white Gaussian noise* (AWGN) with power P_N. Transmit vector $\mathbf{x}[\,i]$ is related to the common information symbol s via linear beamforming, where $\mathbf{w}[\,i] = (w_1[\,i] \ldots w_M[\,i]\,)$ is a beamforming vector that determines the phase that each RS m should apply (before its transmission) on the information intended for the common receiver ($\|\mathbf{w}[\,i]\,\|^2 = 1$ should be verified). Power control is not applied in the array elements, and thus, the total transmit power P_{tx} in the second hop remains fixed during the whole duration of the communication.

The received SNR that the main receiver experiences at transmission time interval i is then given by the following:

$$\gamma[\,i] = \frac{|\mathbf{h}[\,i] \cdot \mathbf{w}[\,i]\,|^2\, \mathbb{E}\{|s|^2\}}{P_N} = \left| \sum_{m=1}^{M} \sqrt{\overline{\gamma}_m[\,i]}\, w_m[\,i]\; e^{j\psi_m[i]} \right|^2, \tag{2}$$

where

$$\overline{\gamma}_m[\,i] = \frac{P_{\text{tx}}}{L_m[\,i]\; P_N} \qquad m = 1, \ldots, M \tag{3}$$

represents the mean received SNR from the mth array element, $L_m[\,i]$ is the total path loss attenuation for the mth signal path (i.e., combines distance-dependent average path loss and shadow fading), $\psi_m[\,i]$ is the corresponding channel phase response, and $w_m[\,i] \in \mathbb{C}^{1\times 1}$ is the beamforming weight that the mth array element applies in transmission.

2.1 General assumptions

In our system model, the mean SNR in Equation 3 is assumed to be invariant in a time scale that is proportional to the duration of a data session (since all RSs in the second hop admit a fixed location). Thus, the channel is considered not to change significantly in time, and therefore, $\overline{\gamma}_m[\,i] = \overline{\gamma}_m$, $\psi_m[\,i] = \psi_m$ is assumed. Based on the time invariant nature of the system, we can also ignore the time index i from the weights $w_m[\,i]$'s (that are used to perform phase adjustments at the mth element of the antenna array). In the presence of channel gains that remain static during the whole duration of the data session, the feedback messages for phase adjustments at the different RSs can spread over an appropriate time span (i.e., $i = 1, 2, \ldots, I$). Thus, the presented performance analysis considers the resulting sum channel when all phase adjustments have been appropriately performed (i.e., after I time intervals of the sequential DBF algorithm that is implemented).

It is also assumed that phases ψ_m are samples of *independent and identically distributed* (i.i.d.) uniform *random variables* (RVs), taking values in the interval $(-\pi, \pi)$.

The performance of the proposed DBF algorithm is studied over a random initial phase configuration (i.e., with no *a priori* information). To fulfill the accurate timing requirements at each element of the disperse antenna array, we assume that each RS in the cluster is able to monitor standard synchronization signals either from the destination (i.e., the main receiver) in the reverse link or from the source (i.e., the main transmitter) in the forward link [17].

If the proposed DBF system is not properly designed, the signal phase shifts that each individual array element apply may create a frequency selective behavior in the equivalent channel that results in the second hop (i.e., increased multipath effect). Yet, in our system model, we assume that the elements of the antenna array are perfectly synchronized or that the synchronization error is small compared to the symbol length. As a consequence, the delay spread of the effective channel will not be (considerably) increased in this situation.

2.2 Limited feedback scheme

As shown in Figure 1, in the second hop of the communication link there are M active array elements transmitting the same complex symbols s to the main receiver. In order to maximize the SNR at the main receiver, each array element adjusts its transmitted signal using a complex, individual beamforming weight

$$\begin{aligned} w_m &= \sqrt{\frac{1}{M}}\, e^{-j\phi_m}, \quad \phi_m \in \mathcal{Q}, \\ \mathcal{Q} &= \left\{ \frac{(2\,n-1)\,\pi}{2^N} : \; n = 1, \ldots, 2^N \right\}, \end{aligned} \tag{4}$$

where N is the number of feedback bits per array element. We note that the individual power per antenna is selected as a long-term parameter, based on the number of active array elements; thus, the total transmit power in the second hop of the system is always equal to P_{tx}, and a fair comparison among results is feasible. The error-free signaling indicating the best index for beamforming weight $w_m \in \mathcal{Q}$ is provided through a dedicated feedback channel in the reverse link.

The selection of phases ϕ_m's is done at the main receiver and is carried out as follows:

1. The receiver first estimates the phases ψ_m from each element of the distributed antenna array, using a specific signal as reference.
2. It then selects the phases ϕ_m from quantization set $\mathcal{Q}$ such that $|\theta_m| = |\phi_m - \psi_m|$ is minimized.

As a result, adjusted phases θ_m will be uniformly i.i.d. in the interval $\left(-\pi/2^N, \pi/2^N\right)$ [20]. Thus, phase adjustments are done independently, using a common phase reference at the receiver side.

3 Performance analysis

In this paper, three different performance measures that have been extensively studied in the literature are computed [21]:

1. *Ergodic capacity.* It represents the long-term average transmission. It can be achieved implementing coding schemes that span code words over several coherence time intervals of the fading channel (valid for applications with no strict delay constraints).
2. *Outage probability.* It constitutes a more appropriate performance indicator in case of constant-rate delay-limited transmissions, where coding must be carried out over a single channel realization. Represents the probability that an outage occurs within a specified time period because target data rate cannot be achieved within current channel conditions.
3. *Bit error probability.* It identifies the probability of making a wrong estimation (in reception) of the information bit that is being transmitted.

Before starting the computation of the previous performance measures, we need to determine suitable expressions for *probability density function* (PDF) and *cumulative distribution function* (CDF) of the received SNR in the second hop. According to the system model presented in section 2, the expression for SNR attains the following form:

$$\gamma[\,i] = |H[\,i]\,|^2 = \frac{1}{M}\left|\sum_{m=1}^{M}\sqrt{\overline{\gamma}_m}\,e^{j\theta_m[i]}\right|^2, \tag{5}$$

where individually received SNRs $\left\{\overline{\gamma}_m : m = 1,\ldots,M\right\}$ are known and remain constant due to the static location of transmitters and receiver during the whole duration of communication. Since we want to analyze the effect of feedback signaling resolution (i.e., N) and the number of elements in the antenna array (i.e., M) in the performance of the DBF system, suitable expressions for the PDF $f\left(\gamma[\,i]\,|\overline{\gamma}_1,\ldots,\overline{\gamma}_M\right)$ and CDF $F\left(\gamma[\,i]\,|\overline{\gamma}_1,\ldots,\overline{\gamma}_M\right)$ are required. Unfortunately, a treatable closed-form expression for these distributions can only be obtained for very specific situations (i.e., not for all values of M and N). However, since in this paper we are interested in studying performance when the number of elements in the distributed antenna array is high (i.e., when $M \geq 10$), we will use the central limit theorem to show that RV presented in Equation 5 can be accurately approximated as the sum of two independent *chi-squared* (χ^2) distributed RVs (one central and one non-central), each with one degree of freedom.

3.1 PDF approximation for a large number of array elements

Due to the Euler's formula, the RV

$$H[\,i] = \sqrt{P_{\text{tx}}/P_N}\left(\mathbf{h}[\,i]\cdot\mathbf{w}[\,i]\,\right) = \widetilde{X}_R[\,i] + j\widetilde{X}_I[\,i] \tag{6}$$

can be written in terms of its real and imaginary parts, with

$$\begin{aligned}\widetilde{X}_R[\,i] &= \sqrt{\frac{1}{M}}\sum_{m=1}^{M}\sqrt{\overline{\gamma}_m}\cos(\theta_m[\,i]\,),\\ \widetilde{X}_I[\,i] &= \sqrt{\frac{1}{M}}\sum_{m=1}^{M}\sqrt{\overline{\gamma}_m}\sin(\theta_m[\,i]\,).\end{aligned} \tag{7}$$

Based on the fact that M is *large*, we use the central limit theorem to claim that both real and imaginary parts of $H[\,i]$ are Gaussian with means μ_R and μ_I, respectively [22]. Since the imaginary part of $H[\,i]$ is a sum of sine functions with symmetrically distributed phases, its mean equals zero (i.e., individual phases $\theta_m[\,i]$ are uniformly i.i.d. in interval $(-\pi/2^N, \pi/2^N)$ for all m, and the sine function is an odd function). Similarly, it is possible to show that the expected value of the real part of $H[\,i]$ is non-negative (actually, $\mu_R = 0$ only when N=0). Based on the discussion presented in the Appendix, we claim that it is possible to approximate RV $|\widetilde{X}_I[\,i]\,|^2$ as a central χ^2 distribution with 1 degree of freedom and RV $|\widetilde{X}_R[\,i]\,|^2$ as a non-central χ^2 distribution with 1 degree of freedom and non-centrality parameter s_1^2 (unknown for the moment). Finally, the parameters that are required to use the proposed approximation for the PDF and CDF of the received SNR can be obtained from the first two raw moments of RVs $\widetilde{X}_R[\,i]$ and $\widetilde{X}_I[\,i]$, whose closed-form expressions are obtained through simple but tedious computations:

$$\mu_R = \sqrt{\frac{1}{M}}\,C_N\sum_{m=1}^{M}\sqrt{\overline{\gamma}_m}, \qquad \mu_I = 0, \tag{8}$$

$$\begin{aligned}\mathbb{E}\left\{\widetilde{X}_R^2\right\} = \frac{1}{M}\Bigg[&\sum_{m=1}^{M}\overline{\gamma}_m\left(\frac{1}{2}+\frac{1}{2}C_{N-1}\right)\\ &+2\sum_{l=1}^{M-1}\sum_{m=l+1}^{M}\sqrt{\overline{\gamma}_l}\sqrt{\overline{\gamma}_m}\,{C_N}^2\Bigg],\end{aligned} \tag{9}$$

and

$$\mathbb{E}\left\{\widetilde{X}_I^2\right\} = \frac{1}{M}\sum_{m=1}^{M}\overline{\gamma}_m\left(\frac{1}{2} - \frac{1}{2}C_{N-1}\right), C_N = \left(\frac{2^N}{\pi}\right)\sin\left(\frac{\pi}{2^N}\right). \tag{10}$$

As shown in the Appendix, the PDF for the received SNR that our DBF algorithm provides (i.e., $Z = |X_R|^2 + |X_I|^2$) can be now expressed as a weighted sum of non-central χ^2 PDFs, i.e.,

$$f_Z(z) = \sum_{k=0}^{\infty} W_k(\sigma_1, \sigma_2) f_k(z) \qquad z \geq 0, \tag{11}$$

where

$$\sigma_1 = \sqrt{\mathbb{E}\left\{\widetilde{X}_R^2\right\} - {\mu_R}^2}, \qquad \sigma_2 = \sqrt{\mathbb{E}\left\{\widetilde{X}_I^2\right\}}, \tag{12}$$

are the standard deviations of the real and imaginary parts of Equation 6, respectively ,

$$W_k(\sigma_1, \sigma_2) = \left(\frac{\sigma_1}{\sigma_2}\right)\frac{\Gamma\left(\frac{1}{2}+k\right)}{\Gamma(k+1)\,\Gamma(\frac{1}{2})}\left(\frac{\sigma_2^2 - \sigma_1^2}{\sigma_2^2}\right)^k \tag{13}$$

is the corresponding weighting factor, and

$$f_k(z) = \frac{1}{2\sigma_1^2}\left(\frac{z}{s_1^2}\right)^{\frac{k}{2}}\exp\left(-\frac{s_1^2 + z}{2\sigma_1^2}\right)\mathcal{I}_k\left(\frac{s_1}{\sigma_1^2}\sqrt{z}\right) \quad z \geq 0 \tag{14}$$

is a non-central χ^2 PDF with $2(k+1)$ degrees of freedom and non-centrality parameter ${s_1}^2 = {\mu_R}^2$, and $\mathcal{I}_k$ is the kth order modified Bessel function of the first kind (see the Appendix for more details). As seen in Figure 2, the weighting factor presented in Equation 13 is only significantly different from zero for low values of k; therefore, only a few terms of the sum in Equation 11 are needed to obtain an accurate approximation for the resulting PDF.

Following a similar procedure, the corresponding CDF for the received SNR can be expressed as a weighted sum of non-central χ^2 CDFs, i.e.,

$$F_Z(z) = \sum_{k=0}^{\infty} W_k(\sigma_1, \sigma_2) F_k(z) \qquad z \geq 0, \tag{15}$$

where

$$F_k(z) = 1 - Q_{k+1}\left(\frac{s_1}{\sigma_1}, \frac{\sqrt{z}}{\sigma_1}\right) \qquad z \geq 0 \tag{16}$$

is the closed-form expression for a non-central χ^2 CDF with $2(k+1)$ degrees of freedom and non-centrality parameter ${s_1}^2$, and $Q_M(a,b)$ is the generalized Marcum Q-function of order M [23].

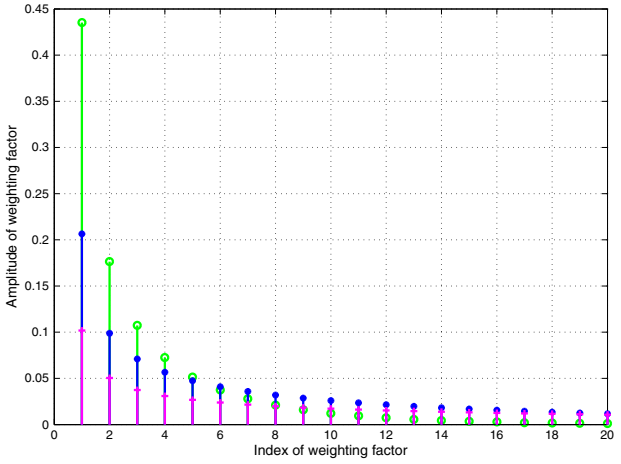

Figure 2 Amplitude of different weighting factor $W_k(\sigma_1, \sigma_2)$'s. They are used to approximate the PDF/CDF of the received SNR $\gamma[i]$ as a weighted sum of non-central χ^2 PDFs/CDFs with different degrees of freedom. Channel phase resolutions (bit/RS): N=1 (o), N=2 (•), and N=3 (+).

3.2 Outage probability

To evaluate the performance of a mobile communication system in practice, it is usually assumed that transmission is successful if the SNR that is observed in reception (for the given transmission time interval) is good enough, or equivalently, if the received SNR value is above a given threshold. In other words, transmission to a given user is said to be feasible if its instantaneous received SNR satisfies the following:

$$\gamma[i] \geq \gamma_0, \tag{17}$$

where the threshold γ_0 is selected to guarantee a certain quality of service (for the given transmission rate). In this situation, the statistical performance requirement

$$\Pr\{\gamma[i] \leq \gamma_0\} = \Pr_{\text{out}}(\gamma_0) \tag{18}$$

is defined as the outage probability of the mobile communication system, for the given target SNR value γ_0. Note that the closed-form CDF expression derived in Equations 15 and 16 can be used to compute the outage probability of the system in a straightforward way.

3.3 Ergodic capacity

The ergodic capacity [23] is defined as follows:

$$C(\overline{\gamma}) = \mathbb{E}\{\log_2(1+\overline{\gamma}z)\} = \int_0^{\infty}\log_2(1+\overline{\gamma}z) f_Z(z)\,dz, \tag{19}$$

where

$$\overline{\gamma} = \frac{P_{\text{tx}}}{P_N} \tag{20}$$

is a reference average SNR for the second hop of our distributed antenna system and

$$z = |\mathbf{h}[\,i\,]\cdot\mathbf{w}[\,i\,]\,|^2 \tag{21}$$

can be approximated as the sum of two χ^2 distributions, a central and a non-central one, with 1 degree of freedom in both cases (see Section 3.1 for more details).

3.3.1 No channel signaling

When there is no channel signaling (i.e., N=0), it is possible to see that the PDFs of both RVs $\widetilde{X}_R$ and $\widetilde{X}_I$ follow a Gaussian distribution with zero mean and identical variance (i.e., ${\sigma_1}^2 = {\sigma_2}^2 = \sigma^2$). Since these RVs can be interpreted as the real and imaginary components of a circularly symmetric complex Gaussian RV, it is possible to conclude that RV Z will be exponentially distributed according to the following:

$$f_Z(z) = \beta e^{-\beta z}, \qquad \beta = \frac{1}{2\sigma^2}. \tag{22}$$

Then, plugging Equation 22 in Equation 19 and using relation derived in Appendix C of [24], we get the following:

$$C(\overline{\gamma}) = \log_2(\bar{\gamma}) + \log_2(e)\left[\exp\left(\frac{1}{2\sigma^2\overline{\gamma}}\right)E_1\left(\frac{1}{2\sigma^2\overline{\gamma}}\right) - \log_e(\overline{\gamma})\right], \tag{23}$$

where

$$E_1(z) = \int_z^\infty \frac{e^{-t}}{t}\,dt \tag{24}$$

is the exponential integral function of the first order [25].

3.3.2 Limited channel signaling

In the presence of limited channel signaling (i.e., when $N \geq 1$), the previous analysis does not hold anymore. Thus, to find a suitable closed-form expression in this situation, we plug approximation (11) in Equation 19, i.e.,

$$C(\overline{\gamma}) = \sum_{k=0}^{\infty} W_k(\sigma_1,\sigma_2)\int_0^\infty \log_2\,(1+\overline{\gamma}z)\,f_k(z)\,dz, \tag{25}$$

where the weighting factor $W_k(\sigma_1,\sigma_2)$ is defined in Equation 13 and the non-central χ^2 PDF $f_k(z)$ is presented in Equation 14. Since the exact computation of Equation 25 is not simple in this situation, a well-known approximation is used instead. It is known that when an RV is concentrated near its mean, Jensen's approximation

$$\mathbb{E}\{g(z)\} \leq g(\mathbb{E}\{z\}) \tag{26}$$

gets particularly accurate when '$g(\cdot)$' is a concave function [22]. To analyze the degree of variability of RV Z around its mean, we propose to use the following fading figure:

$$\mathcal{F}_Z = \frac{\mathbb{E}^2\{Z\}}{Var\{Z\}}, \tag{27}$$

where

$$\mathbb{E}\{Z\} = \mathbb{E}\{\widetilde{X}_R^2\} + \mathbb{E}\{\widetilde{X}_I^2\} \tag{28}$$

can be computed with the aid of closed-form expressions derived in Equations 9 and 10; see reference [24] for more details. It can be seen from Table 1 that the values of fading figures are always larger than 1, and they tend to grow as M and N increase. The only exception is the case N=0, where no coherent combining gain is possible due to the absence of channel feedback information to carry out the co-phasing procedure in transmission; thus, in this particular situation, the fading figure parameter takes values close to 1 in all cases (and tends asymptotically to the unitary value since the central limit theorem starts to work in a better way when the number of distributed antenna elements M grows large). It is important to highlight that case N=0 was analyzed separately in Section 3.3.1, following a different approach with respect to the case where limited channel signaling is available.

Therefore, closed-form approximation

$$\begin{aligned} C(\overline{\gamma}) &= \mathbb{E}\left\{\log_2(e)\log_e\left[\overline{\gamma}\left(\frac{1}{\overline{\gamma}}+z\right)\right]\right\} \\ &\cong \log_2(e)\left[\log_e(\overline{\gamma}) + \log_e\left(\frac{1}{\overline{\gamma}}+\mathbb{E}\{z\}\right)\right] \end{aligned} \tag{29}$$

results, providing a good solution for feedback resolutions that verify $N \geq 1$. Actually,closed-form formula (29) provides a strict upper bound for the ergodic capacity, which becomes asymptotically optimal as the channel phase resolution grows large (i.e., as $N \to \infty$).

3.4 Bit error probability

The average bit error probability can be expressed using

$$\overline{P}_e = \int_0^\infty P_{mod}\,(\overline{\gamma}z)\,f_Z(z)dz, \tag{30}$$

where $f_Z(z)$ is the PDF of the instantaneous SNR and

$$P_{mod}\,(\bar{\gamma}z) = Q\left(\sqrt{2\overline{\gamma}z}\right) = \frac{1}{2}\mathrm{erfc}\left(\sqrt{\overline{\gamma}z}\right) \tag{31}$$

is the error rate when the modulation scheme is BPSK.

Table 1 Fading figure values of received SNR in the presence of different *N* and *M*

Feedback resolutions	*M*=10	*M*=20
$N=0$	1.112	1.053
$N=1$	12.62	23.18
$N=2$	262.0	521.4
$N=3$	4475.5	9037.6

When $f_Z(z)$ is the PDF of a non-central χ^2 distributed RV with n degrees of freedom, the average BEP can be written as follows:

$$P_e(M) = P_e(M-1) - \frac{1}{2}\binom{2M-2}{M-1} \times \sqrt{\frac{d}{1+d}}\left[\frac{1}{4(1+d)}\right]^{M-1} \times \exp\left(-\frac{\kappa d}{1+d}\right) K\left(\frac{1}{2}, M; -\frac{\kappa}{1+d}\right) M > 1, \tag{32}$$

where $M = n/2$ is the multichannel order,

$$\kappa = \frac{s^2}{2\sigma^2} \tag{33}$$

is the ratio between the energy of the deterministic component and the average received energy via the random component

$$d = \sigma^2 \bar{\gamma}, \tag{34}$$

and

$$K(a, c; z) = \sum_{n=0}^{\infty} \frac{(a)_n}{(c)_n} \frac{z^n}{n!} \tag{35}$$

is the confluent hypergeometric function, where

$$(b)_n = \frac{\Gamma(b+n)}{\Gamma(b)} \tag{36}$$

is the so-called Pochhammer's symbol (also known as rising factorial) [25]. When M=1, the error rate is given by

$$P_e(1) = Q(u, w) - \frac{1}{2}\left[1 + \sqrt{\frac{d}{1+d}}\right] \exp\left(-\frac{u^2+w^2}{2}\right) \mathcal{I}_0(uw), \tag{37}$$

where

$$u = \sqrt{\frac{\kappa\left[1 + 2d - 2\sqrt{d(1+d)}\right]}{2(1+d)}}, \quad w = \sqrt{\frac{\kappa\left[1 + 2d + 2\sqrt{d(1+d)}\right]}{2(1+d)}}. \tag{38}$$

For more details, see [26].

Based on the previous formulas, it is possible to show that the BEP that the distributed antenna system provides in the second hop, when the SNR at the main receiver is approximated as a weighted sum of non-central χ^2 distributions with different degrees of freedom, attains the following closed-form expression:

$$P_e = \sum_{k=0}^{\infty} W_k(\sigma_1, \sigma_2) P_e(k+1), \tag{39}$$

where $P_e(k+1)$ is obtained from Equation 32 to Equation 38, while weighting factor $W_k(\sigma_1, \sigma_2)$ is given in Equation 13.

4 Numerical results

In this section, we analyze the performance of the proposed (coherent) DBF algorithm based on the previously presented analyses. We investigate the corresponding outage probability, ergodic capacity, and bit error probability for different amounts of channel phase signaling (i.e., diverse N), for different channel amplitude models (dependent on the physical location of the cooperative network elements), and for various numbers of active RSs (i.e., diverse M).

Regarding the long-term part of the channel model, we consider that the mean received SNRs from the different array elements $\overline{\gamma}_m$'s are assumed to be fixed over the whole duration of the data communication. In addition, in those cases where array elements are grouped into two different clusters (with exactly half the number of active array elements in each one), we use the notation

$$\delta = \frac{\overline{\gamma}_{(1)}}{\overline{\gamma}_{(2)}} \tag{40}$$

to represent the power imbalance situation between both groups. Here, $\overline{\gamma}_{(1)}$ and $\overline{\gamma}_{(2)}$ represent the individual average SNRs of the active array elements in the first cluster (stronger channel gains) and the second cluster (weaker channel gains), respectively. The channel amplitudes from different array elements in the second hop are random samples of a Rayleigh distribution, with unitary second raw moment. This is equivalent to say that the individual instantaneous SNR values (observed from each of the array elements in the second hop) are considered to be exponential i.i.d. RVs, with unitary mean value $\overline{\gamma}_m = 1$.

4.1 Outage probability

Figure 3 shows the outage probability for a given SNR threshold, when using the proposed DBF algorithm for different amounts of channel phase signaling in presence of M=10 active array elements. Rayleigh distributed channel amplitudes have been used to model the stochastic behavior of the channel in this situation. Solid lines are plotted based on approximation (15) with appropriate fitting parameters, along with asymptotic upper bounds in case of full CSI at array elements (dashed line). Note that in this paper, full CSI is actually a synonym of perfect channel phase information, since no channel amplitude information is considered to be available at the transmitter side (i.e., RS are always transmitting with constant power). In all cases, simulated point values (*) are also included to verify the validation of the analytical results. According to these results, we see that the proposed approximation follows simulated values well. For larger numbers of active

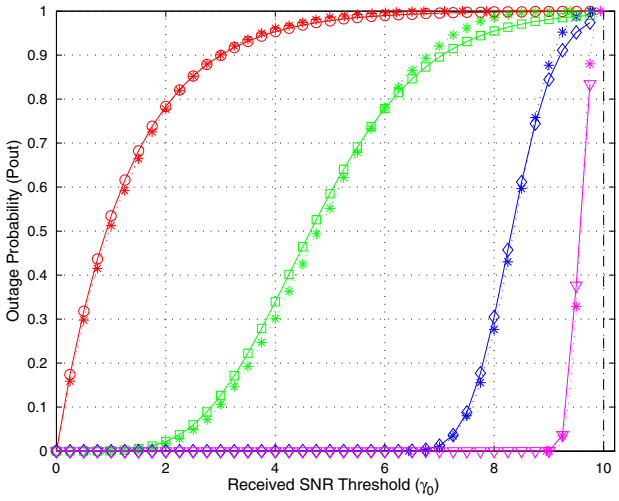

Figure 3 Outage probability as a function of SNR threshold γ_0 for a DBF with $M = 10$ array elements. Solid lines: no CSI (○), N=1 (□), N=2 (◇), N=3 (∇). Dashed-dotted line denotes full CSI at array elements. Simulated values are denoted by (*). Channel amplitudes from different array elements in the second hop are random samples of a Rayleigh distribution, with unitary second raw moment (i.e., $\overline{\gamma}_m = 1$).

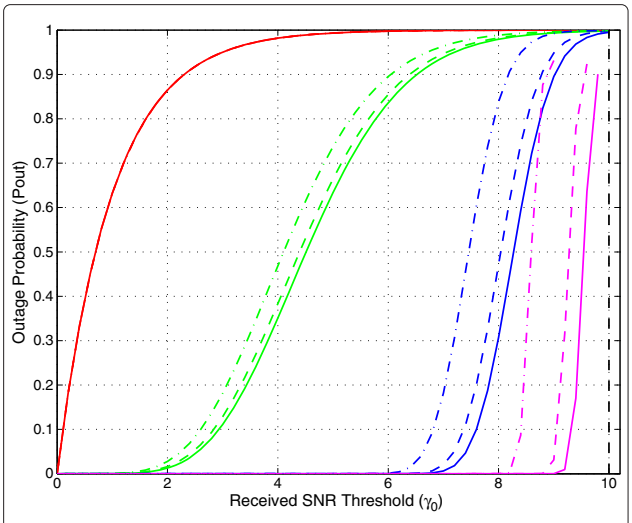

Figure 4 Outage probability as a function of SNR threshold γ_0 for DBF with 10 array elements. Solid lines: perfect channel power balance (i.e., $\delta = 0$ dB). Dashed lines: medium channel power imbalance (i.e., $\delta = 3$ dB). Dotted lines: large channel power imbalance (i.e., $\delta = 6$ dB). Channel feedback: no CSI (red), N=1 (green), N=2 (blue), and N=3 (magenta). Dashed-dotted line (black): full CSI at array elements. Channel amplitudes are fixed according to the different channel power imbalance situations.

array elements (e.g., when M=20), the obtained approximation shows a similar behavior with better accuracy (the figures that show this behavior are not included since they do not bring new insights in the main matter of the paper). In Figure 3, the outage probability in absence of channel phase signaling is used as a baseline. It is found that performance in terms of outage probability clearly increases with additional phase bits in the feedback link. We also note that if N=3, then the performance of DBF algorithm is very close to the one observed with full CSI at the elements of the distributed antenna array.

Figure 4 shows the outage probability for a given SNR threshold when implementing the DBF algorithm in different channel power imbalance situations in the presence of M=10 active array elements. In this case, array elements are grouped in two clusters (of the same size) that are located at different distances from the main receiver. Note that mean received SNR values for different antenna elements were selected to guarantee the same performance for different channel power imbalance situations, in the absence of signaling information (this is the reason why different performance curves overlap for different channel power imbalance situations when N=0). Solid lines, dashed lines, and dotted lines represent perfect channel power balance (i.e., $\delta = 0$ dB), medium channel power imbalance (i.e., $\delta = 3$ dB), and high channel power imbalance (i.e., $\delta = 6$ dB) situations, respectively. Based on the results, we observe that the power imbalance level in the channel amplitude model increases the outage probability of the DBF algorithm. The larger the number of phase bits N, the larger is this the impairment in absolute values. The same behavior is visible when the number of active array elements increases (again, these figures are not included since those results are similar to the ones that are observed in Figure 4). As expected, in the presence of individual channel gains with different average path loss characteristics (i.e., with different long-term signal strength), the variability of the received SNR increases at the main receiver, causing a less abrupt improvement in the sigmoid function of the CDF as the value of γ_0 grows.

Finally, Figure 5 presents the maximum SNR threshold that can be guaranteed for a given outage probability when implementing the proposed DBF algorithm in a perfect channel power balance case (i.e., when $\delta = 0$ dB). These curves admit almost linear behavior with respect to the number of active array elements M. Based on these curves, we observe that the gap between the different outage probability curves decreases as N grows. This is in accordance with the behavior of the expected value of the real part of the sum channel (i.e., μ_R), given in Equation 8 and presented in Figure 6.

4.2 Ergodic capacity

Figures 7 and 8 show the ergodic capacity as a function of the number of active array elements (i.e., M) and phase feedback bits per network element (i.e., N), respectively. Again, (constant) Rayleigh i.i.d. samples were used

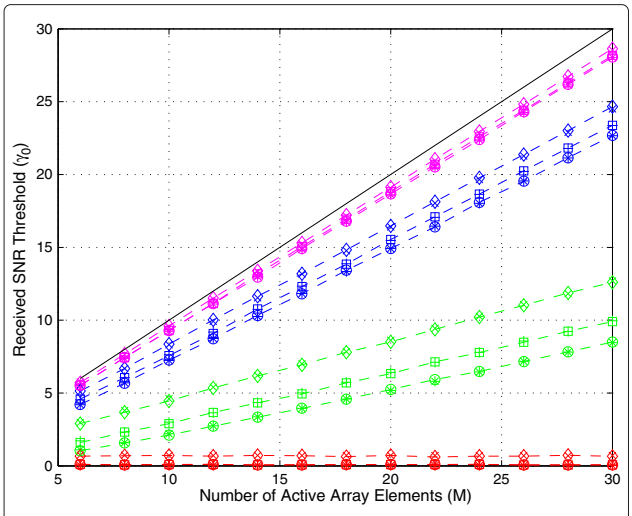

Figure 5 Required SNR threshold γ_0 for DBF to guarantee a given outage probability. It is presented a function of the number active array elements. Outage probability: $\Pr_{\text{out}} = 0.02$ (∘), $\Pr_{\text{out}} = 0.1$ (□), and $\Pr_{\text{out}} = 0.5$ (◇). Channel feedback: no CSI (red), N=1 (green), N=2 (blue), and N=3 (magenta). Solid (black) line: full CSI at array elements. Simulated values are denoted by (*). Channel amplitudes are fixed with perfect power balance.

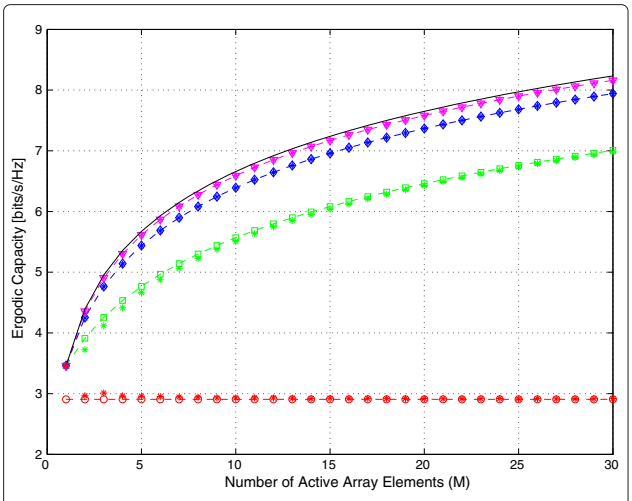

Figure 7 Ergodic capacities for different numbers of phase bits. They are presented as a function of the number of active array elements when the average SNR $\overline{\gamma} = 10$ dB. Dashed lines represent the following theoretical curves: N=0 (∘), N=1 (□), N=2 (◇), and N=3 (▽). Solid (black) line: full CSI at RSs. Simulated values are denoted by (*). Channel amplitudes are fixed with perfect power balance.

to model the individual channel amplitudes in the second hop. In the case of limited channel phase signaling, the curves were plotted based on approximation (26). In the absence of channel phase signaling (i.e., for N=0), the closed-form expression (23) was used. Simulated point values (*) are also included to verify the accuracy of the approximation that was proposed to estimate the values of the ergodic capacity in the different situations. Note that, as expected, the ergodic capacity performance increases when both the resolution of the channel phase information and the number of cooperative network elements grow. The solid (black) line in Figure 7 represents the asymptotic upper bound with full CSI at the RSs. Note that the proposed approximation provides results very close to the theoretical upper bound, even when the channel phase feedback resolution takes values as low as N=3 bits/RS.

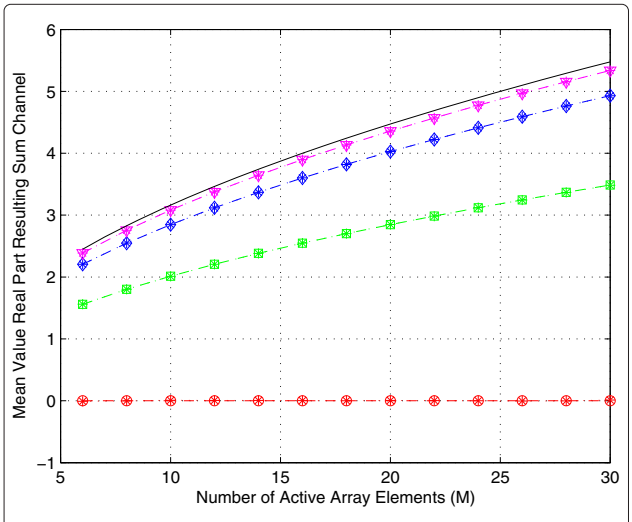

Figure 6 Expected value for the real part of the sum channel μ_R. It is presented as a function of the number active array elements. Dashed lines: no CSI (∘), N=1 (□), N=2 (◇), and N=3 (▽). Solid (black) line: full CSI at array elements. Simulated values are denoted by (*). Channel amplitudes are fixed with perfect power balance.

4.3 Bit error probability

Figure 9 presents the BEP curves that are achieved when implementing our DBF algorithm with different amounts of channel phase signaling resolution in the second hop. Dashed lines and dotted lines represent the theoretical and simulated DBF models, respectively. The solid (black) line represents the BEP lower bound situation, achieved when using BPSK modulation in an equivalent AWGN channel model. According to these results, it is possible to conclude that the proposed theoretical model approximates simulated results of our DBF architecture in an accurate way. It is also straightforward to see that, when the number of phase bits exceeds N=2 bits/RS, the proposed approximated methods provide a BEP curve that is very close to the one that corresponds to an equivalent AWGN channel model (i.e., lower bound for our BEP analysis). Note that these simulation results support the previously presented claim (for both outage probability and ergodic capacity analyses) that the use of channel

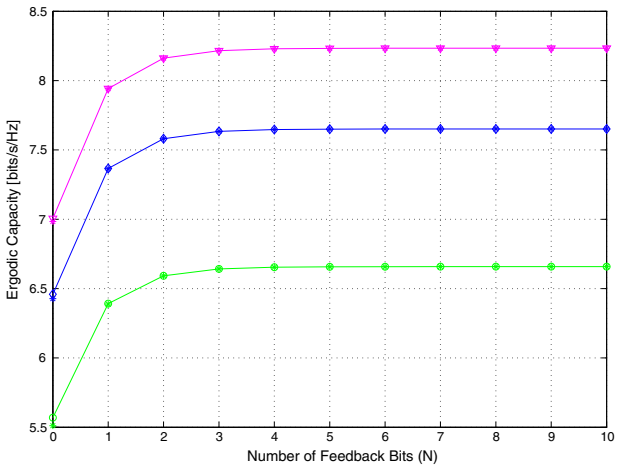

Figure 8 Ergodic capacities for different number of active array elements. They are presented as a function of the number of phase bits when the average SNR $\overline{\gamma} = 10$ dB. Solid lines represent the theoretical curves: M=10 (□), $M = 20$ (◇), and M=30 (▽). Simulated values are denoted by (*). Channel amplitudes are fixed with perfect power balance.

phase resolution exceeding N=3 bits/RS does not provide additional improvements in the end-to-end performance of our DBF architecture.

In the light of all results, we conclude that there is no reason to use more than N=3 bits/RS to implement a DBF algorithm in a cooperative wireless scenario, provided that the number of cooperative antennas is large enough. Yet, the performance that is obtained with N=1 bit/RS is not good enough. However, the performance obtained with N=2 bits/RS provides a reasonable trade-off between *the cost* of signaling overhead and *the benefit* that the improvement in the different performance measures under analysis (i.e., outage probability, ergodic capacity, and bit error probability) represents.

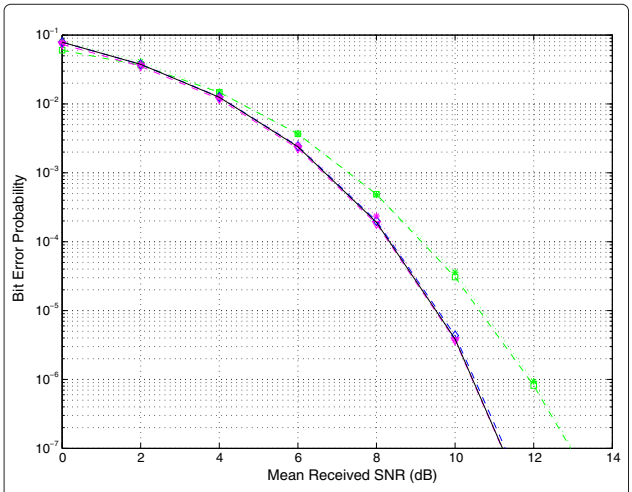

Figure 9 Bit error probabilities for different number of phase bits. The number of active array elements is $M = 20$. Dashed lines represent the theoretical models: N=1 (□), N=2 (◇), and N=3 (∇). Simulated values denoted by dotted lines with (*). Solid (black) line represents the AWGN channel lower bound. Channel amplitudes are fixed with perfect power balance.

5 Conclusions

We studied the performance of a DBF algorithm in the presence of different amounts of channel phase feedback information. This analysis was done in the context of a wireless communication system, where the subscriber (main transmitter) receives assistance from a cooperative cluster of network elements that boosts its communication to the macro-base station (main receiver). This cooperative network is formed by a large number of low-cost array elements deployed in the close proximity of the transmitter (e.g., the same room or office). Location of the array elements was assumed to be fixed during the whole duration of data transmission. Due to short distances, the communication over the first hop (i.e., from main transmitter to elements of the distributed array) was assumed to be costless in terms of transmission power and radio resource usage. Therefore, the bottleneck of the system model was assumed to be in the second hop (i.e., from the elements of the disperse antenna array to the main receiver).

Three different performance measures were used to study the performance of the DBF algorithm: outage probability, ergodic capacity, and bit error probability. To carry out the analysis, suitable closed-form approximations for the PDF and the CDF of the received SNR in the second hop were derived. The parameters for the approximations were obtained from the first two raw moments of the resulting sum channel that the main receiver observes. With the aid of these PDF and CDF expressions, useful closed-form formulas for the selected performance parameters were derived. All these approximations were validated using numerical simulations. Our analysis revealed that notable gains can be achieved in all performance measures when using a small amount of phase feedback information in the DBF algorithm that is configured in the second hop of our cooperative system scenario.

Appendix

PDF and CDF for sum of χ^2 distributions

Let $\{X_l\}_{l=1}^{n}$ be independent Gaussian RVs with common variance σ^2 and non-negative mean μ_l. Then, it is possible to show that sum

$$Y = \sum_{l=1}^{n} {X_l}^2 \tag{41}$$

follows a *non-central* χ^2 distribution with n degrees of freedom [23]. The corresponding PDF expression is given by

$$f_{\mathrm{nc}n,}(y) = \frac{1}{2\sigma^2}\left(\frac{y}{s^2}\right)^{\frac{n-2}{4}} \exp\left(-\frac{s^2+y}{2\sigma^2}\right) \mathcal{I}_{\frac{n}{2}-1}\left(\frac{s}{\sigma^2}\sqrt{y}\right) \quad y \geq 0, \tag{42}$$

where

$$s^2 = \sum_{l=1}^{n} \mu_l^2 \tag{43}$$

is the non-centrality parameter of the distribution and

$$\mathcal{I}_\alpha(x) = \frac{1}{2\pi}\int_{-\pi}^{\pi} \cos(\alpha\theta)\exp(x\cos\theta)d\theta \tag{44}$$

is the αth order modified Bessel function of the first kind [25]. It is known that the characteristic function of non-central χ^2 distributed RV is defined in closed-form and is given by

$$\Psi_{\mathrm{nc}n,}(\omega) = \left(\frac{1}{1-2j\omega\sigma^2}\right)^{\frac{n}{2}} \exp\left(\frac{j\omega s^2}{1-2j\omega\sigma^2}\right). \tag{45}$$

When all means of RVs $\{X_l\}_{l=1}^n$ are zero (i.e., when $\mu_l = 0$ for $l = 1,\ldots,n$), the distribution of RV (41) reduces to a *central* χ^2 distribution, whose PDF expression for n degrees of freedom is given by

$$f_{\mathrm{c},n}(y) = \frac{1}{2^{\frac{n}{2}}\Gamma\left(\frac{n}{2}\right)\sigma^n} y^{\frac{n}{2}-1}\exp\left(-\frac{y}{2\sigma^2}\right) \quad y \geq 0, \tag{46}$$

where

$$\Gamma(y) = \int_0^\infty t^{y-1}\exp(-t)\,dt \tag{47}$$

represents the Gamma function [23]. The characteristic function in this situation is given by

$$\Psi_{\mathrm{c},n}(\omega) = \left(\frac{1}{1-2j\omega\sigma^2}\right)^{\frac{n}{2}}. \tag{48}$$

Let us now assume that

$$Z = Y_1 + Y_2 \tag{49}$$

is the combination of two independent χ^2 RVs: a non-central χ^2 RV with non-centrality parameter ${s_1}^2$ and variance ${\sigma_1}^2$, and a central χ^2 RV with variance ${\sigma_2}^2$.Let us consider that the degrees of freedom are equal in both cases (i.e., $n_1 = n_2 = n$). Then, the characteristic function [22]

$$\Psi_{Z,n}(\omega) = \Psi_{\mathrm{nc}n,}(\omega)\,\Psi_{\mathrm{c}n,}(\omega) = \left[\frac{1}{\left(1-2j\omega{\sigma_1}^2\right)\left(1-2j\omega{\sigma_2}^2\right)}\right]^{\frac{n}{2}} \exp\left(\frac{j\omega{s_1}^2}{1-2j\omega{\sigma_1}^2}\right) \tag{50}$$

can be inverse-Fourier transformed to yield the following closed-form PDF expression:

$$f_{Z,n}(z) = \frac{1}{2{\sigma_1}^2}\left(\frac{\sigma_1}{\sigma_2}\right)^n \left(\frac{z}{{s_1}^2}\right)^{\frac{n-1}{2}} \exp\left(-\frac{z+{s_1}^2}{2{\sigma_1}^2}\right) \times \left\{\sum_{k=0}^{\infty}\frac{\Gamma\left(\frac{n}{2}+k\right)}{\Gamma(k+1)\,\Gamma\left(\frac{n}{2}\right)}\left[\frac{\sqrt{z}\left({\sigma_2}^2-{\sigma_1}^2\right)}{s_1{\sigma_2}^2}\right]^k \mathcal{I}_{n+k-1}\left(\frac{\sqrt{z}s_1}{{\sigma_1}^2}\right)\right\} \quad z \geq 0. \tag{51}$$

When the degree of freedom of both χ^2 RVs are unitary (i.e., when $n_1 = n_2 = 1$), it is possible to show that the closed-form expression for the PDF of RV Z can be written as a weighted sum of non-central χ^2 distributions with different degrees of freedom, i.e.,

$$f_Z(z) = \sum_{k=0}^{\infty} W_k(\sigma_1,\sigma_2) f_{\mathrm{nc}2(k+1),}(z) \qquad z \geq 0, \tag{52}$$

where

$$W_k(\sigma_1,\sigma_2) = \left(\frac{\sigma_1}{\sigma_2}\right)\frac{\Gamma\left(\frac{1}{2}+k\right)}{\Gamma(k+1)\,\Gamma\left(\frac{1}{2}\right)}\left(\frac{\sigma_2^2-\sigma_1^2}{\sigma_2^2}\right)^k \tag{53}$$

is the corresponding weighting factor and $f_{\mathrm{nc}2(k+1),}(z)$ is the non-central χ^2 distribution presented in (42), where $2(k+1)$ are the degrees of freedom of the different terms of the sum. It is also possible to show that the CDF in this situation admit the following form:

$$F_{Z,n}(z) = \left(\frac{\sigma_1}{\sigma_2}\right)^n \sum_{k=0}^{\infty}\frac{\Gamma\left(\frac{n}{2}+k\right)}{\Gamma(k+1)\Gamma\left(\frac{n}{2}\right)}\left(\frac{{\sigma_2}^2-{\sigma_1}^2}{{\sigma_2}^2}\right)^k \times\left[1-Q_{n+k}\left(\frac{s_1}{\sigma_1},\frac{\sqrt{z}}{\sigma_1}\right)\right] \qquad z \geq 0, \tag{54}$$

where

$$Q_M(a,b) = \int_b^\infty x\left(\frac{x}{a}\right)^{M-1}\exp\left(-\frac{x^2+a^2}{2}\right)\mathcal{I}_{M-1}(ax)dx \tag{55}$$

is the generalized Mth order Marcum Q-function [23]. In similar fashion to a previously presented PDF expansion, it is also possible to show that the CDF of RV Z (when $n_1 = n_2 = 1$) can be written as a weighted sum of non-

central χ^2 distributions with different degrees of freedom, i.e.,

$$F_Z(z) = \sum_{k=0}^{\infty} W_k(\sigma_1, \sigma_2) F_{\mathrm{nc}2(k+1)}, (z) \qquad z \geq 0, \quad (56)$$

where

$$F_{\mathrm{nc}n}, (z) = 1 - Q_{n/2}\left(\frac{s_1}{\sigma_1}, \frac{\sqrt{z}}{\sigma_1}\right) \qquad z \geq 0 \quad (57)$$

is the CDF of a non-central χ^2 distributed RV with n degrees of freedom and parameters ${s_1}^2$ and ${\sigma_1}^2$.

Abbreviations

AWGN: Additive white Gaussian noise; BS: Base station; CDF: Cumulative distribution function; CSI: Channel state information; DAS: Distributed antenna system; DBF: Distributed Beamforming; DF: Decode-and-forward; FBS: Femto-base station; i.i.d.: Independent and identically distributed; MBS: Macro-base station; PDF: Probability density function; RS: Relaying station; RV: Random variable; SINR: Signal-to-interference-plus-noise power ratio; SNR: Signal-to-noise power ratio; UE: User equipment.

Competing interests

The authors declare that they have no competing interests.

Author's information

JH received his M.Sc. and Ph.D. degrees from the University of Oulu, Finland, in 1992 and 1998, respectively. From 1999 to the end of 2007, he was with Nokia and Nokia Siemens Networks where he worked on various aspects of mobile communication systems. Since 2008, he has been a professor in the Department of Communications and Networking in Aalto University. His current research interests include multi-antenna transmission and reception techniques, scheduling, relays, small cells, and design and analysis of wireless networks in general. He is an author or co-author to around 130 scientific publications and 35 US patents or patent applications. AAD was born in San Nicolas, Province of Buenos Aires, Argentina in 1978. He received his degree in telecommunications engineering from Blas Pascal University, Cordoba, Argentina in 2002 and his Ph.D. degree from the National University of Cordoba, Argentina in 2010. From 2003 to 2009, he has been with the Digital Communications Research Laboratory, National University of Cordoba, Argentina, carrying out research in the area of MIMO wireless communications. Since the beginning of 2010, he has been working at the Department of Communications and Networking, Aalto University, Finland, taking a position as post-doctoral researcher. His current research interests lie in the area of interference management for future wireless networks, including multi-antenna schemes, time- and frequency-domain scheduling, and power control techniques. TH was born in Kokkola, Finland in 1982. He received his M.Sc. degree from the University of Oulu, Finland in 2010 and his Licentiate degree from Aalto University, Finland in 2013. He has been working as a researcher at Aalto University since 2010 at the Department of Communications and Networking. His main research interests are in the field of cooperative communication, particularly of distributed beamforming in the context of wireless access network.

Acknowledgements

This work was prepared in NETS2020 and SMAS project frameworks and was supported in part by Finnish Funding Agency for Technology and Innovation, Academy of Finland (under grant 133652), Nokia Siemens Networks, Ericsson Finland, Nokia, and Nethawk. This paper was presented in part at the First International Conference on Performance, Safety and Robustness in Complex Systems and Applications (PESARO) 2011.

Author details

[1]Department of Communications and Networking, Aalto University, P.O. Box 13000, Aalto FI-00076, Finland. [2]Ericsson R&D Center, Elektroniikkatie 10, Oulu FI-90590, Finland.

Received: 21 June 2012 Accepted: 18 March 2013
Published: 26 April 2013

References

1. ITU, Assessment of the global mobile broadband deployments and forecasts for international mobile telecommunications. Report ITU-R M.2243 (00/2011), ITU (2011), pp. 1–96
2. Ericsson, More than 50 billion connected, devices. White paper, Ericsson, 1–12 (2011)
3. S Liu, J Wu, CH Koh, V Lau, A 25 Gb/s(/km^2) Urban wireless network beyond IMT-advanced. IEEE Commun. Mag. **49**(2), 122–129 (2011)
4. AA Dowhuszko, T Halinen, J Hämäläinen, O Tirkkonen, in *Proceedings of the First International Conference on Performance, Safety and Robustness in Complex Systems and Applications, (PESARO)*. Performance of relay-aided distributed beamforming techniques in presence of limited feedback information (IARIA, Budapest, Hungary, April 17–22, 2011, pp. 28–34
5. G Mansfield, in *Femto Cells Europe*. Femtocells in the US market–business drivers and consumer propositions AT&T, June 2008), pp. 23–25
6. R Pabst, B Walke, D Schultz, P Herhold, H Yanikomeroglu, S Mukherjee, H Viswanathan, M Lott, W Zirwas, M Dohler, H Aghvami, DD Falconer, GP Fettweis, Relay-based deployment concepts for wireless and mobile broadband radio. IEEE Commun. Mag. **42**(9), 80–89 (2004)
7. M Husso, J Hämäläinen, R Jänti, J Li, E Mutafungwa, R Wichman, Z Zheng, AM Wyglinski, Interference mitigation by practical transmit beamforming methods in closed femtocells. EURASIP J. Wireless Commun. Netw. **2010**, 1–12 (2010)
8. V Chandrasekhar, J Andrews, A Gatherer, Femtocell networks: a survey. IEEE Commun. Mag. **46**(9), 59–67 (2008)
9. M Kuhn, S Berger, I Hammerstom, A Wittneben, Power line enhanced cooperative wireless communications. IEEE J. Sel. Areas Commun. **24**(7), 1401–1410 (2006)
10. H Li, J Hajipour, A Attar, VCM Leung, Efficient HetNet implementation using broadband wireless access with fiber-connected massively distributed antennas architecture. IEEE Commun. Mag. **18**(3), 72–78 (2011)
11. A Özgür, OD Lévêque, NC Tse, Hierarchical cooperation achieves optimal capacity scaling in ad hoc networks. IEEE Trans. Inform. Theory. **53**(10), 3549–3572 (2007)
12. Q Li, RQ Hu, Y Qian, G Wu, Cooperative communications for wireless networks: techniques and applications in LTE-advanced systems. IEEE Wireless Commun. **19**(2), 22–29 (2012)
13. Z Ding, WH Chin, K Leung, Distributed beamforming and power allocation for cooperative networks. IEEE Trans. Wireless Commun. **7**(5), 1817 –1822 (2008)
14. X Chen, S Song, K Letaief, in *Proceedings of IEEE International Conference on Communications*. Transmit and cooperative beamforming in multi-relay systems (IEEE Cape Town, South Africa, 23–27 May 2010), pp. 1–5
15. R Mudumbai, D Brown, U Madhow, H Poor, Distributed transmit beamforming: challenges and recent progress. IEEE Commun. Mag. **47**(2), 102–110 (2009)
16. Y Jing, B Hassibi, Distributed space-time coding in wireless relay networks. IEEE Trans. Wireless Commun. **5**(12), 3524–3536 (2006)
17. D Gesbert, S Hanly, H Huang, S Shamai, O Simeone, W Yu, Multi-cell MIMO cooperative networks: a new look at interference. IEEE J. Sel. Areas Comm. **28**(9), 1380–1408 (2010)
18. R Mudumbai, G Barriac, U Madhow, On the feasibility of distributed beamforming in wireless networks. IEEE Trans. Wireless Commun. **6**(5), 1754 –1763 (2007)
19. L Lei, Z Zhong, C Lin, X Shen, Operator controlled device-to-device communications in LTE-advanced networks. IEEE Wireless Commun. **19**(3), 96–104 (2012)
20. J Hämäläinen, R Wichman, AA Dowhuszko, G Corral-Briones, Capacity of generalized UTRA FDD closed-loop transmit diversity modes. Wireless Pers. Commun. **54**(3), 467–484 (2010)

21. E Biglieri, J Proakis, S Shamai, Fading channels: information-theoretic and communications aspects. IEEE Trans. Inf. Theory. **44**(6), 2619 –2692 (1998)
22. A Papoulis, *Probability, Random Variables, and Stochastic Processes*, 3rd edn. (McGraw-Hill, New York, 1991)
23. JG Proakis, *Digital Communications*, 4th edn. (McGraw-Hill, New York, 2001)
24. AA Dowhuszko, G Corral-Briones, J Hämäläinen, R Wichman, On throughput-fairness tradeoff in virtual MIMO systems with limited feedback. EURASIP. J. Wireless Commun. Netw. **2009**, 1–17 (2009)
25. M Abramowitz, IA Stegun, *Handbook of Mathematical Functions: With Formulas, Graphs, and Mathematical Tables*. (Dover Publications, New York, 1970)
26. WC Lindsey, Error probabilities for Rician fading multichannel reception of binary and N-ary signals. IEEE Trans. Inf. Theory. **10**(4), 339–350 (1964)

doi:10.1186/1687-6180-2013-88
Cite this article as: Halinen *et al.*: Performance of distributed beamforming for dense relay deployments in the presence of limited feedback information. *EURASIP Journal on Advances in Signal Processing* 2013 **2013**:88.